Journal of Sound and Vibration (2002) **258**(2), 359–372
doi:10.1006/jsvi.5141, available online at http://www.idealibrary.com on IDEAL®

DYNAMIC BEHAVIOUR OF A SINGLE-SPAN BEAM SUBJECTED TO LOADS MOVING WITH VARIABLE SPEEDS

G. T. Michaltsos

National Technical University of Athens, 42, Patission street, Athens 10682, Greece.
E-mail: michalts@central.ntua.gr

(*Received* 21 *September* 2001)

This paper deals with the linear dynamic response of a simply supported elastic single-span beam subjected to a moving load of constant magnitude and variable velocity. This analysis focuses attention on the effect of the acceleration or deceleration on the behaviour of the beam under a single (one-axle) load, or a real vehicle model (two-axle load), while the influence of the damping of the beam is taken into account for this last model. A variety of numerical results allows us to draw important conclusions for structural design purposes.

1. INTRODUCTION

The determination of the dynamic effect of moving loads on elastic structures and, particularly, on bridges is a very complicated problem. This multi-parameter problem has been studied by many researchers, in order to present reliable solutions. For this purpose two different methods are used: The first one is to perform tests and the second is that of pure theoretical investigation.

The problem of moving loads was first considered approximately for the case of a girder with negligible mass, compared to the mass of a single moving load of constant magnitude by Stokes [1] and Zimmermann [2]. Afterwards, the case of a moving load with negligible mass compared to the mass of the girder was studied by Krylov [3], Timoshenko [4] and Lowan [5].

The complete problem, including both these parameters, was studied by other investigators such as Steuding [6], Schallemcamp [7], and Bolotin [8]. A very thorough treatise on the dynamic response of several types of railway bridges, traversed by steam locomotives was presented by Inglis [9] using harmonic analysis. Interesting analyses were also presented by Hillerborg [10] using Fourier's analysis and by Biggs *et al.* [11] using Iglis's technique. The problem of the dynamic response of bridges under moving loads is reviewed in detail by Timoshenko [12], and later on by Kolousek [13]. One should also mention the extended review reported by Fryba [14] in his excellent monograph on this subject. Based on his text, Fryba [15, 16] studied the effects of the constant speed and damping on the response of a beam.

Many investigators ascertained that some parameters, usually neglected, had an interesting, and often pronounced, influence on the dynamic behaviour of the bridges. One can mention, for example, the type of the vehicle Veletsos and Huang [17], the mass of the moving load Michaltsos *et al.* [18], the constants of the springs and dampers Fertis [19], the bridge's uneven deck Abdel-Rohman and Al Duaij [20], Michaltsos and

0022-460X/02/$35.00

Konstantakopoulos [21], the centripetal and Coriolis forces Michaltsos and Kounadis [22] and many others.

A very important parameter in the study of the vibration of bridges caused by moving loads is the velocity. Although there is scarcity of publications on this subject, one must mention the work of Zibdeh [23] who included the effect of random velocities on the dynamic response of a bridge traversed by a concentrated load.

The present paper examines the influence of random loads moving with variable speeds on the dynamic behaviour of a single-span beam. Three cases are considered. Firstly, the concentrated load, moved with time-varying velocity, secondly the vehicle (with wheelbase equal to $2d$), moving also with time-varying velocity and finally, the influence of light damping (with coefficient c) on the above case of a moving vehicle. The approach is based on the Euler–Bernoulli's beam theory. Closed form solutions for the mean and variance of the deflection are obtained and comparison of the results for the aforementioned three cases is performed.

2. MATHEMATICAL FORMULATION

Consider the simply supported beam, shown in Figure 1, of length ℓ, having a prismatic cross-section with constant mass per unit length m, flexural rigidity EI and rotational inertia J_b made from linear, homogeneous and isotropic material. The beam is traversed by a mass-load $P = M\mathbf{g}$, with rotational inertia J_v, subjected to the horizontal force $F(t)$ and moving with the velocity $v(t)$.

The position α of the mass-load from the left end of the beam at any time t is equal to $a = s(t)$, where t is measured from the instant the load enters the span. Before that instant, the deflections throughout the length of the beam are assumed to be zero. The equations of motion are

$$EI\,w'''' + c_e\dot{w} + c_i\dot{w}'''' - 2J_b\ddot{w}'' + m\ddot{w} = M[\mathbf{g} - (\ddot{w} + \ddot{s}w' + 2\dot{s}\dot{w}' + \dot{s}^2w'')]\delta(x-\alpha) + J_v\ddot{w}'\delta'(x-\alpha), \tag{1}$$

$$M\ddot{s} + M\ddot{w}w'\delta(x-\alpha) = F(t), \tag{2}$$

where the prime denotes differentiation with respect to x, while the dot to time t, $\mathbf{g}$ is the gravitational acceleration and $\delta(x-\alpha)$ the Dirac function.

The associated boundary and initial conditions are, respectively

$$w(0,t) = w(\ell,t) = w''(0,t) = w''(\ell,t) = 0, \tag{3}$$

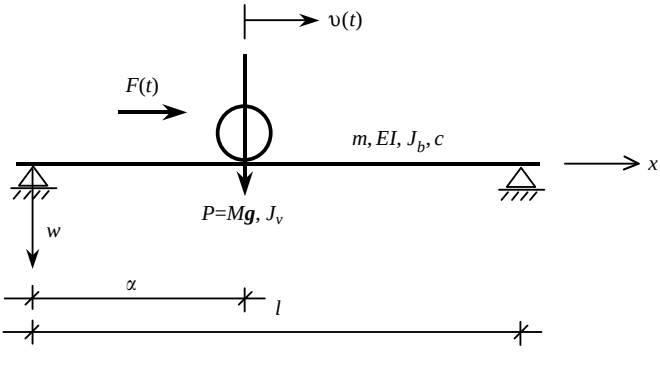

Figure 1. A single-span beam traversed by an one-axle load.

and

$$w(x,0) = \dot{w}(x,0) = 0. \tag{4}$$

In the present paper, one is interested in movements with

$$F(t) = F = \text{constant} \tag{5}$$

and therefore

$$\ddot{s} = \gamma = \text{constant}, \quad \dot{s} = \upsilon = \upsilon_0 + \gamma t, \quad s = \upsilon_0 t + \gamma t^2/2, \tag{6}$$

where γ is the acceleration or deceleration of the moving mass-load, $\upsilon = \upsilon(t)$ its velocity and $\upsilon_0 = \text{constant}$, the initial velocity at time $t = 0$ when the mass-load enters the beam.

2.1. THE CONCENTRATED LOAD

The simplest and more usual case is of a moving load without consideration of the influence of inertia forces (like mass, or centripetal and Coriolis forces whose influence has already been determined in references [18, 22]). This leads to

$$EI\, w''''(x,t) + m\ddot{w}(x,t) = M\mathbf{g}\delta(x-a). \tag{7}$$

A series solution of equation (7) in terms of linear normal modes can be sought in the form

$$w(x,t) = \sum_n w_n(x,t) = \sum_n X_n(x) T_n(t), \tag{8}$$

where

$$X_n(x) = \sin(n\pi x/\ell), \quad (n = 1, 2, \cdots). \tag{9}$$

Substituting equation (8) into equation (7), multiplying the result by $X_n(x)$, integrating over the domain, and considering the orthogonality condition, the differential equation of the nth mode of the generalized deflection can be written as

$$\ddot{T}_n + \omega_n^2 T_n = (2M\mathbf{g}/m\ell)\sin[(n\pi/\ell)(\upsilon_0 t + \gamma t^2/2)], \quad \text{for } \gamma > 0, \tag{10a}$$

$$T_n + \omega_n^2 T_n = (2M\mathbf{g}/m\ell)\sin[(n\pi/\ell)(\upsilon_0 t - \gamma t^2/2)], \quad \text{for } \gamma < 0, \tag{10b}$$

where

$$\omega_n^2 = \frac{n^4\pi^4 EI}{m\ell^4}, \quad (n = 1, 2, \cdots) \tag{11}$$

are the eigenfrequencies of the beam.

The solution of equation (10) is given by the Duhamel's formula as

$$T_n = \frac{2M\mathbf{g}}{m\ell\omega_n}\left\{\int_0^t \sin\frac{n\pi\upsilon_0\tau}{\ell}\cos\frac{n\pi\gamma\tau^2}{2\ell}\sin\omega_n(t-\tau)\,\mathrm{d}\tau + \int_0^t \cos\frac{n\pi\upsilon_0\tau}{\ell}\sin\frac{n\pi\gamma\tau^2}{2\ell}\sin\omega_n(t-\tau)\,\mathrm{d}\tau\right\}, \quad \gamma > 0, \tag{12a}$$

$$T_n = \frac{2M\mathbf{g}}{m\ell\omega_n}\left\{\int_0^t \sin\frac{n\pi\upsilon_0\tau}{\ell}\cos\frac{n\pi\gamma\tau^2}{2\ell}\sin\omega_n(t-\tau)\,\mathrm{d}\tau - \int_0^t \cos\frac{n\pi\upsilon_0\tau}{\ell}\sin\frac{n\pi\gamma\tau^2}{2\ell}\sin\omega_n(t-\tau)\,\mathrm{d}\tau\right\}, \quad \gamma < 0, \tag{12b}$$

For the second case (deceleration) one notes that the vehicle stops at

$$t = \upsilon_0/\gamma, \quad \ell > \upsilon_0^2/2\gamma, \tag{13a}$$

$$t = 1/\gamma(\upsilon_0 - \sqrt{\upsilon_0^2 - 2\gamma\ell}), \quad \ell < \upsilon_0^2/2\gamma. \tag{13b}$$

2.2. THE MOVING VEHICLE

One considers the vehicle of Figure 2, having the characteristics: (a) Number of axes, 2; (b) mass, M; (c) length of wheelbase, $2d$; (d) distance of its gravity centre from the upper surface of the bridge deck, h; (e) moving force, $F = M\gamma$; (f) acceleration (or deceleration) produced by F, γ.

One assumes that the first (front) axis enters the beam at $t = 0$ and that for a vehicle at rest ($\upsilon = 0$) the load $P = M\mathbf{g}$ is divided equally between the two axles of the vehicle. Hence the forces P_1 and P_2 can be expressed as

$$P_1 = \frac{M\mathbf{g}}{2} - \frac{M\gamma h}{2d}, \quad P_2 = \frac{M\mathbf{g}}{2} + \frac{M\gamma h}{2d}, \ \gamma > 0, \tag{14}$$

$$P_1 = \frac{M\mathbf{g}}{2} + \frac{M\gamma h}{2d}, \quad P_2 = \frac{M\mathbf{g}}{2} - \frac{M\gamma h}{2d}, \ \gamma < 0 \tag{15}$$

On the other hand, since the second (back) wheel enters the bridge at time t_d, while the front wheel will have traversed a distance $2d$ one can write $2d = \upsilon_0 t_d + \gamma t_d^2/2$ giving

$$t_d = 1/\gamma(-\upsilon_0 + \sqrt{\upsilon_0^2 + 4\gamma d}), \ \gamma > 0, \tag{16}$$

$$t_d = 1/\gamma(\upsilon_0 - \sqrt{\upsilon_0^2 + 4\gamma d}), \ \gamma < 0. \tag{17}$$

At $t = t_d$, the back wheel will be entering the bridge at a speed

$$\upsilon_d = \upsilon_0 + \gamma t_d, \ \gamma > 0, \tag{18}$$

$$\upsilon_d = \upsilon_0 - \gamma t_d, \ \gamma < 0, \tag{19}$$

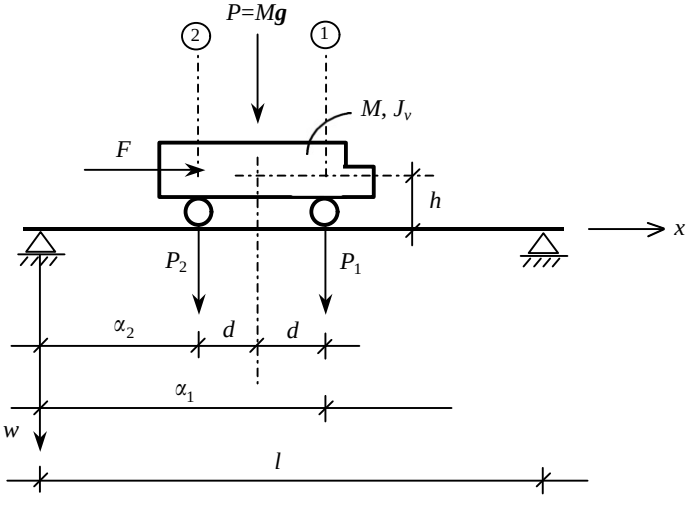

Figure 2. A single-span beam traversed by a two-axle vehicle.

The front wheel, at time t, will arrive at a point that is, distance α_1 from the entrance of the bridge such that

$$\alpha_1 = v_0 t + \gamma t^2/2, \quad \gamma > 0, \tag{20}$$

$$\alpha_1 = v_0 t - \gamma t^2/2, \quad \gamma < 0. \tag{21}$$

The back wheel will arrive at time $t - t_d$ (time from its entry on the bridge) at a point that is, distance α_2 from the entrance of the bridge such that

$$\alpha_2 = (v_0 + \gamma t_d)(t - t_d) + \frac{\gamma (t - t_d)^2}{2}, \quad \gamma > 0, \tag{22}$$

$$\alpha_2 = (v_0 - \gamma t_d)(t - t_d) - \frac{\gamma (t - t_d)^2}{2}, \quad \gamma < 0 \tag{23}$$

Then equation (8) becomes

$$EI\, w'''' + m\ddot{w} = P_1 \delta(x - \alpha_1) + P_2 \delta(x - \alpha_2). \tag{24}$$

A solution is sought with the form

$$w(x, t) = \sum_n X_n(x) T_n(t), \tag{25}$$

where $X_n(x)$ is given by equation (9).

Comparing equations (24) and (25)

$$EI \sum_n X_n'''' \, T_n + m \sum_n X_n \ddot{T}_n = \frac{M}{2}\left(\mathbf{g} - \frac{\gamma h}{d}\right)\delta(x - \alpha_1) + \frac{M}{2}\left(\mathbf{g} + \frac{\gamma h}{d}\right)\delta(x - \alpha_2), \quad \gamma > 0,$$

and since X_n satisfies the equation of free vibration, one may finally write

$$\sum_n X_n \ddot{T}_n + \sum_n \omega_n^2 X_n T_n = \frac{M}{2m}\left(\mathbf{g} - \frac{\gamma h}{d}\right)\delta(x - \alpha_1) + \frac{M}{2m}\left(\mathbf{g} + \frac{\gamma h}{d}\right)\delta(x - \alpha_2), \quad \gamma > 0. \tag{26}$$

Multiplying both sides by X_n, integrating the results over the domain and taking into account the orthogonality condition, we get

$$\ddot{T}_n + \omega_n^2 T_n = \Gamma_n(t), \tag{27}$$

where

$$\begin{aligned}\Gamma_n = {} & \frac{M}{m\ell}\left(\mathbf{g} - \frac{\gamma h}{d}\right)\left(\sin\frac{n\pi v_0 t}{\ell}\cos\frac{n\pi\gamma t^2}{2\ell} + \cos\frac{n\pi v_0 t}{\ell}\sin\frac{n\pi\gamma t^2}{2\ell}\right) \\ & + \frac{M}{m\ell}\left(\mathbf{g} + \frac{\gamma h}{d}\right)\left\{\sin\frac{n\pi(v_0 + \gamma t_d)(t - t_d)}{\ell}\cos\frac{n\pi\gamma(t - t_d)^2}{2\ell}\right. \\ & \left. + \cos\frac{n\pi(v_0 + \gamma t_d)(t - t_d)}{\ell}\sin\frac{n\pi\gamma(t - t_d)^2}{2\ell}\right\}\mathrm{H}(t - t_d), \quad \gamma > 0, \end{aligned} \tag{28}$$

$$\Gamma_n = \frac{M}{m\ell}\left(\mathbf{g} + \frac{\gamma h}{d}\right)\left(\sin\frac{n\pi v_0 t}{\ell}\cos\frac{n\pi\gamma t^2}{2\ell} - \cos\frac{n\pi v_0 t}{\ell}\sin\frac{n\pi\gamma t^2}{2\ell}\right)$$
$$+\frac{M}{m\ell}\left(\mathbf{g} - \frac{\gamma h}{d}\right)\left\{\sin\frac{n\pi(v_0 - \gamma t_d)(t - t_d)}{\ell}\cos\frac{n\pi\gamma(t - t_d)^2}{2\ell}\right.$$
$$\left.-\cos\frac{n\pi(v_0 - \gamma t_d)(t - t_d)}{\ell}\sin\frac{n\pi\gamma(t - t_d)^2}{2\ell}\right\}\mathrm{H}(t - t_d),\quad \gamma < 0 \tag{29}$$

with $\mathrm{H}(t - t_d)$ as Heaviside's function.

The solution of equation (27) is given by Duhamel's integral as

$$T_n(t) = \frac{1}{\omega_n}\int_0^t \Gamma_n(\tau)\sin\omega_n(t - \tau)\,\mathrm{d}\tau. \tag{30}$$

The calculation of integrals (30) is given in Appendix A.

2.3. THE MOVING VEHICLE WITH DAMPING

Equation (24), in this case, becomes

$$EI\,w'''' + c\dot{w} + m\ddot{w} = P_1\delta(x - \alpha_1) + P_2\delta(x - \alpha_2). \tag{31}$$

Following the same procedure as in section 2.2, and for a solution in the form $w = \sum X_n T_n$,

$$\ddot{T}_n + (c/m)\dot{T}_n + \omega_n^2 T_n = (2P_1/m\ell)\sin\frac{n\pi\alpha_1}{\ell} + (2P_2/m\ell)\sin\frac{n\pi\alpha_2}{\ell}. \tag{32}$$

The solution of the above equation (32) is given by Duhamel's second integral as

$$T_n = \frac{2P_1}{m\ell\omega_n^*}\int_0^t \sin\left[\frac{n\pi}{\ell}\left(v_0\tau + \frac{\gamma\tau^2}{2}\right)\right]\mathrm{e}^{-\beta(t-\tau)}\sin\omega_n^*(t - \tau)\,\mathrm{d}\tau$$
$$+\frac{2P_2}{m\ell\omega_n^*}\int_0^t \sin\left\{\frac{n\pi}{\ell}\left[(v_0 + \gamma t_d)(\tau - t_d) + \frac{\gamma(\tau - t_d)^2}{2}\right]\right\}$$
$$\mathrm{e}^{-\beta(t-\tau)}\sin\omega_n^*(t - \tau)\mathrm{H}(\tau - t_d)\,\mathrm{d}\tau,\quad \gamma > 0, \tag{33}$$

$$T_n = \frac{2P_1}{m\ell\omega_n^*}\int_0^t \sin\left[\frac{n\pi}{\ell}\left(v_0\tau - \frac{\gamma\tau^2}{2}\right)\right]\mathrm{e}^{-\beta(t-\tau)}\sin\omega_n^*(t - \tau)\,\mathrm{d}\tau$$
$$+\frac{2P_2}{m\ell\omega_n^*}\int_0^t \sin\left\{\frac{n\pi}{\ell}\left[(v_0 - \gamma t_d)(\tau - t_d) - \frac{\gamma(\tau - t_d)^2}{2}\right]\right\}$$
$$\mathrm{e}^{-\beta(t-\tau)}\sin\omega_n^*(t - \tau)\mathrm{H}(\tau - t_d)\,\mathrm{d}\tau,\quad \gamma < 0, \tag{34}$$

where

$$\beta = c/2m,\quad \omega^* = \sqrt{\omega_n^2 - \beta^2} \tag{35}$$

and P_1, P_2 are given by equations (14) and (15).

2.4. DIMENSIONLESS FORMS

Using the dimensionless parameters

$$\xi = x/\ell,\ \ \zeta = \gamma/\mathbf{g},\ \ T_1 = (2/\pi)\sqrt{m\ell^4/EI},\ \ \tau = t/T_1,\ \ \bar{h} = h/\ell,\ \ \bar{d} = d/\ell,\ \ \tau_d = t_d/T_1,$$
$$\bar{c} = (c/2m)\ T_1,\ \ \bar{\upsilon} = \upsilon T_1/\ell,\ \ \bar{\gamma} = \gamma(T_1^2/\ell),\ \ \bar{M} = M/m\ell,\ \ \bar{\upsilon}_0 = \upsilon_0 T_1/\ell, \tag{36}$$

one can write

$$\Omega_n t = n\pi\bar{\upsilon}\tau,\ \ \omega_n t = 2n^2\pi\tau,\ \ \Omega_n/\omega_n = \bar{\upsilon}/2n,\ \ \bar{\upsilon} = \bar{\upsilon}_0 + \bar{\gamma}\tau,\ \ \omega_n = 2n^2\pi/T_1,$$
$$\Omega_n = n\pi\bar{\upsilon}/T_1,\ \ n\pi\gamma t^2/2\ell = n\pi\bar{\gamma}\tau^2/2,\ \ \omega_n^* = 1/T_1\sqrt{4n^4\pi^2 - \bar{c}^2},\ \ \bar{\beta} = \bar{c}/T_1. \tag{37}$$

Finally, the dimensionless nth mode displacement $\bar{w}_n(\xi,\tau)$ of the beam, is given in sections 2.4.1–2.4.3.

2.4.1. *The concentrated load*

$$\bar{w}_n(\xi,\tau) = w_n(x,t)/(\mathbf{g}m\ell^4/\pi^3 EI) = (4\bar{M}/n^2)\sin(n\pi\xi)\bar{T}_n(\tau), \tag{38}$$

where

$$\bar{T}_n = \int_0^\tau \sin(n\pi\bar{\upsilon}_0\tau^*)\cos\frac{n\pi\bar{\gamma}\tau^{*2}}{2}\sin[2n^2\pi(\tau-\tau^*)]\,\mathrm{d}\tau^* + \int_0^\tau \cos(n\pi\bar{\upsilon}_0\tau^*)\sin\frac{n\pi\bar{\gamma}\tau^{*2}}{2}\sin[2n^2\pi(\tau-\tau^*)]\,\mathrm{d}\tau^*,\ \ \gamma > 0, \tag{39}$$

$$\bar{T}_n = \int_0^\tau \sin(n\pi\bar{\upsilon}_0\tau^*)\cos\frac{n\pi\bar{\gamma}\tau^{*2}}{2}\sin[2n^2\pi(\tau-\tau^*)]\,\mathrm{d}\tau^* - \int_0^\tau \cos(n\pi\bar{\upsilon}_0\tau^*)\sin\frac{n\pi\bar{\gamma}\tau^{*2}}{2}\sin[2n^2\pi(\tau-\tau^*)]\,\mathrm{d}\tau^*,\quad \gamma<0. \tag{40}$$

2.4.2. *The moving vehicle*

$$\bar{w}_n(\xi,\tau) = w_n(x,t)/(\mathbf{g}m\ell^4/\pi^3 EI) = (2\bar{M}/n^2)\sin(n\pi\xi)\bar{T}_n(\tau), \tag{41}$$

where

$$\begin{aligned}\bar{T}_n = (1-\zeta\bar{h}/\bar{d})&\left[\int_0^\tau \sin(n\pi\bar{\upsilon}_0\tau^*)\cos\frac{n\pi\bar{\gamma}\tau^{*2}}{2}\sin[2n^2\pi(\tau-\tau^*)]\,\mathrm{d}\tau^*\right.\\ &\left.+\int_0^\tau \cos(n\pi\bar{\upsilon}_0\,{}^*\tau)\sin\frac{n\pi\bar{\gamma}\tau^{*2}}{2}\sin[2n^2\pi(\tau-\tau^*)]\,\mathrm{d}\tau^*\right]\\ &+\left(1+\frac{\zeta\bar{h}}{\bar{d}}\right)\left[\int_0^\tau \sin[n\pi(\bar{\upsilon}_0+\bar{\gamma}\tau_d)(\tau^*-\tau_d)]\cos\frac{n\pi\bar{\gamma}(\tau^*-\tau_d)^2}{2}\right.\\ &\times\sin[2n^2\pi(\tau-\tau^*)]\mathrm{H}(\tau^*-\tau_d)\,\mathrm{d}\tau^*\\ &+\int_0^\tau \cos[n\pi(\bar{\upsilon}_0+\bar{\gamma}\tau_d)(\tau^*-\tau_d)]\sin\frac{n\pi\bar{\gamma}(\tau^*-\tau_d)^2}{2}\\ &\left.\times\sin[2n^2\pi(\tau-\tau^*)]\mathrm{H}(\tau^*-\tau_d)\right]\mathrm{d}\tau^*,\ \ \gamma>0,\end{aligned} \tag{42}$$

$$\bar{T}_n = \left(1 + \frac{\zeta\bar{h}}{\bar{d}}\right)\left[\int_0^\tau \sin(n\pi\bar{v}_0\tau^*)\cos\frac{n\pi\bar{\gamma}\tau^{*2}}{2}\sin[2n^2\pi(\tau-\tau^*))]\,\mathrm{d}\tau^*\right.$$
$$\left. - \int_0^\tau \cos(n\pi\bar{v}_0\tau^*)\sin\frac{n\pi\bar{\gamma}\tau^{*2}}{2}\sin[2n^2\pi(\tau-\tau^*)]\,\mathrm{d}\tau^*\right]$$
$$+ \left(1 - \frac{\zeta\bar{h}}{\bar{d}}\right)\left[\int_0^\tau \sin[n\pi(\bar{v}_0 + \bar{\gamma}\tau_d)(\tau^* - \tau_d)]\cos\frac{n\pi\bar{\gamma}(\tau^* - \tau_d)^2}{2}\right.$$
$$\times \sin[2n^2\pi(\tau-\tau^*)]\mathrm{H}(\tau^* - \tau_d)\,\mathrm{d}\tau^*$$
$$\left. - \int_0^\tau \cos[n\pi(\bar{v}_0 + \bar{\gamma}\tau_d)(\tau^* - \tau_d)]\sin\frac{n\pi\bar{\gamma}(\tau^* - \tau_d)^2}{2}\right.$$
$$\left.\times \sin[2n^2\pi(\tau-\tau^*)]\mathrm{H}(\tau^* - \tau_d)\,\mathrm{d}\tau^*\right],\quad \gamma < 0. \tag{43}$$

2.4.3. *The moving vehicle with damping*

$$\bar{w}_n(\xi,\tau) = w_n(x,t)(\mathbf{g}m\ell^4/\pi^3 EI) = \frac{2\bar{M}}{\sqrt{n^4 - (\bar{c}/2\pi)^2}}\sin(n\pi\xi)\bar{T}_n(\tau), \tag{44}$$

where

$$\bar{T}_n = \left(1 - \frac{\zeta\bar{h}}{\bar{d}}\right)\left[\int_0^\tau \sin(n\pi\bar{v}_0\tau^*)\cos\frac{n\pi\bar{\gamma}\tau^{*2}}{2}\sin\left[\sqrt{4n^4\pi^2 - \bar{c}^2}(\tau-\tau^*)\right]\mathrm{e}^{-\bar{c}(\tau-\tau^*)}\,\mathrm{d}\tau^*\right.$$
$$\left. + \int_0^\tau \cos(n\pi\bar{v}_0\tau^*)\sin\frac{n\pi\bar{\gamma}\tau^{*2}}{2}\sin\left[\sqrt{4n^4\pi^2 - \bar{c}^2}(\tau-\tau^*)\right]\mathrm{e}^{-\bar{c}(\tau-\tau^*)}\,\mathrm{d}\tau^*\right]$$
$$+ \left(1 + \frac{\zeta\bar{h}}{\bar{d}}\right)\left[\int_0^\tau \sin[n\pi(\bar{v}_0 + \bar{\gamma}\tau_d)(\tau^* - \tau_d)]\cos\frac{n\pi\bar{\gamma}(\tau^* - \tau_d)^2}{2}\right.$$
$$\times \sin\left[\sqrt{4n^4\pi^2 - \bar{c}^2}(\tau-\tau^*)\right]\mathrm{e}^{-\bar{c}(\tau-\tau^*)}\mathrm{H}(\tau^* - \tau_d)\,\mathrm{d}\tau^*$$
$$\left. + \int_0^\tau \cos[n\pi(\bar{v}_0 + \bar{\gamma}\tau_d)(\tau^* - \tau_d)]\sin\frac{n\pi\bar{\gamma}(\tau^* - \tau_d)^2}{2}\right.$$
$$\left.\times \sin\left[\sqrt{4n^4\pi^2 - \bar{c}^2}(\tau-\tau^*)\right]\mathrm{e}^{-\bar{c}(\tau-\tau^*)}\mathrm{H}(\tau^* - \tau_d)\,\mathrm{d}\tau^*\right],\quad \gamma > 0, \tag{45}$$

$$\bar{T}_n = \left(1 + \frac{\zeta\bar{h}}{\bar{d}}\right)\left[\int_0^\tau \sin(n\pi\bar{v}_0\tau^*)\cos\frac{n\pi\bar{\gamma}\tau^{*2}}{2}\sin\left[\sqrt{4n^4\pi^2 - \bar{c}^2}(\tau-\tau^*)\right]\mathrm{e}^{-\bar{c}(\tau-\tau^*)}\,\mathrm{d}\tau^*\right.$$
$$\left. - \int_0^\tau \cos(n\pi\bar{v}_0\tau^*)\sin\frac{n\pi\bar{\gamma}\tau^{*2}}{2}\sin\left[\sqrt{4n^4\pi^2 - \bar{c}^2}(\tau-\tau^*)\right]\mathrm{e}^{-\bar{c}(\tau-\tau^*)}\,\mathrm{d}\tau^*\right]$$
$$+ (1 - \frac{\zeta\bar{h}}{\bar{d}})\left[\int_0^\tau \sin[n\pi(\bar{v}_o + \bar{\gamma}\tau_d)(\overset{*}{\tau} - \tau_d)]\cos\frac{n\pi\bar{\gamma}(\tau^* - \tau_d)^2}{2}\right.$$
$$\left.\times \sin\left[\sqrt{4n^4\pi^2 - \bar{c}^2}(\tau-\tau^*)\right]\mathrm{e}^{-\bar{c}(\tau-\tau^*)}\mathrm{H}(\tau^* - \tau_d)\,\mathrm{d}\tau^*\right.$$

$$- \int_0^{\tau} \cos[n\pi(\bar{v}_0 + \bar{\gamma}\tau_d)(\tau^* - \tau_d)] \sin \frac{n\pi\bar{\gamma}(\tau^* - \tau_d)^2}{2}$$
$$\times \sin\left[\sqrt{4n^4\pi^2 - \bar{c}^2}(\tau - \tau^*)\right] e^{-\bar{c}(\tau-\tau^*)} H(\tau^* - \tau_d)\, d\tau^*\Big], \quad \gamma < 0. \tag{46}$$

3. NUMERICAL RESULTS AND DISCUSSION

In this section, results in both graphical and tabular form are presented. The effect on the dynamic response of a bridge of a load (or vehicle, see Figure 2) moving with variable speed combined with various parameters such as initial velocity or type of vehicle are discussed in detail.

The mathematical model considered herein is related to a real bridge with a span of $\sim$100 m, weight per unit length of $\sim$150 kN/m and moment of inertia $\sim$0·80 m^4, which is traversed by a moving load with weight 600 kN, moved with initial velocities $v_0 = 0$, 20, 30 and 40 m/s and accelerations (or decelerations) $\gamma = 0$, 3, 6, 9 and 12 m/s^2 or in dimensionless form mass $\bar{M} = 0{\cdot}05$, velocities $\bar{v} = 0$, 0·38, 0·57, and 0·76 and accelerations (or decelerations) $\bar{\gamma} = 0$, 0·11, 0·22, 0·33, and 0·44 respectively. The remaining characteristics are: $h = 1{\cdot}5$ m, $2d = 8$ m, $c = 1250$ Ns/m or in dimensionless form $\bar{h} = 0{\cdot}015$, $2\bar{d} = 0{\cdot}08$, $\bar{c} = 0{\cdot}05$.

Numerical results are given in Tables 1 and 2.

TABLE 1

Dimensionless deflections $w(0{\cdot}5, t)$ for various dimensionless initial velocities $\bar{v}_0$ and accelerations $\bar{\gamma}$, for the cases of an one-axle load, two-axle vehicle and a two-axle vehicle with damping

$\bar{v}$	$\bar{\gamma}$	First one-axle	Second two-axle	Third two-axle damping	2–1 (%)	3–2 (%)
0·00	0·00	—	—	—	—	—
	0·11	0·0365488	0·0331876	0·0328557	−9·19	−1·00
	0·22	0·0375575	0·0328769	0·0324495	−12·46	−1·30
	0·33	0·0382156	0·0367686	0·0362171	−4·03	−1·51
	0·44	0·0380566	0·0391482	0·0385218	+2·87	−1·59
0·38	0·00	0·0367220	0·0314440	0·0318643	−14·37	+1·33
	0·11	0·0374035	0·0336308	0·0337989	−10·08	+0·49
	0·22	0·0409037	0·0368054	0·0367685	−10·02	−0·10
	0·33	0·0435678	0·0395225	0·0392854	−9·28	−0·62
	0·44	0·0455301	0·0418376	0·0414611	−8·11	−0·90
0·57	0·00	0·0472969	0·0394842	0·0395728	−16·52	+0·22
	0·11	0·0490444	0·0416449	0·0413534	−15·09	−0·71
	0·22	0·0502667	0·0435067	0·0428541	−13·45	−0·49
	0·33	0·0510234	0·0450923	0·0444610	−11·62	−0·40
	0·44	0·0516009	0·0464272	0·0460093	−10·03	−0·91
0·76	0·00	0·0543276	0·0468736	0·0466483	−13·72	−0·48
	0·11	0·0547343	0·0478551	0·0471851	−12·57	−1·40
	0·22	0·0548834	0·0487004	0·0479699	−11·26	−1·49
	0·33	0·0548121	0·0494222	0·0489774	−9·83	−0·91
	0·44	0·0545605	0·0500296	0·0496793	−8·30	−0·69

TABLE 2

Dimensionless deflections $w(0.5, t)$ for various dimensionless initial velocities $\bar{v}_0$ and decelerations $\bar{\gamma}$, for the cases of an one-axle load, two-axle vehicle and a two-axle vehicle with damping

$\bar{v}$	$\bar{\gamma}$	First one-axle	Second two-axle	Third two-axis + damping	2–1 (%)	3–2 (%)
0.38	0·00	0·0367220	0·0314440	0·0318643	−14·37	+1·34
	0·11	0·0419286	0·0335010	0·0333330	−20·10	−0·51
	0·22	0·0337591	0·0296601	0·0293635	−12·14	−1·02
	0·33	0·0217150	0·0253288	0·0251261	+16·64	−0·79
	0·44	0·0190705	0·0229527	0·0227989	+20·39	−0·70
0·57	0·00	0·0472969	0·0394842	0·0395728	−16·52	+0·22
	0·11	0·0450186	0·0387695	0·0385368	−13·88	−0·60
	0·22	0·0422641	0·0377349	0·0338859	−10·71	−0·20
	0·33	0·0452819	0·0363593	0·0359957	−19·70	−1·02
	0·44	0·0358255	0·0346354	0·0344622	−3·33	−0·51
0·76	0·00	0·0543276	0·0468736	0·0466483	−13·97	−0·48
	0·11	0·0536316	0·0467086	0·0461481	−12·91	−1·20
	0·22	0·0526227	0·0463936	0·0456977	−11·83	−1·49
	0·33	0·0512902	0·0458992	0·0454861	−10·51	−0·90
	0·44	0·0492876	0·0452018	0·0448853	−8·29	−0·71

In Table 1, the accelerating motion ($\bar{\gamma} > 0$) is comprehensively considered. The dimensionless deflections of the middle of the bridge (at $\xi = 0{\cdot}5$) are determined for the cases of a concentrated moving load of mass $\bar{M}$ (first case), or for a moving vehicle of, also, mass $\bar{M}$ (second case) or, finally, of a moving vehicle of mass $\bar{M}$ with damping coefficient $\bar{c}$ (third case). Percentage increase or decrease of the deflections of the bridge between second and first or third and second cases are determined in the two last columns respectively. In Table 2, the decelerating motion ($\bar{\gamma} < 0$) is also comprehensively considered.

From the plots of Figures 3 and 4 one can see graphically the relationship between the dimensionless time τ and the deflections $\bar{w}$ of the middle of the bridge (at $\xi = 0{\cdot}5$) in conjuction with the dimensionless acceleration (or deceleration) $\bar{\gamma}$. Figure 3, is concerned with the accelerating movement and shows in: column 1 the movement of an one-axle load-mass $\bar{M}$, column 2 the movement of a two-axle vehicle of mass $\bar{M}$, and column 3 the movement of the above two-axle vehicle including damping.

Figure 4 concerns the decelerating movement with columns 1, 2, and 3 describing the same cases as in Figure 3.

Figure 5 shows the relationship between the dimensionless acceleration (or deceleration, dashed lines) $\bar{\gamma}$ and the dimensionless deflections $\bar{w}$ (at $\xi = 0{\cdot}5$) of the middle of the bridge in connection with the dimensionless initial speed $\bar{v}_0$.

From the above plots, it can be comprehensively concluded:

(a) The model of the single axle is not accurate, compared with the two-axle example (the given results from the one-axle model are more unfavourable).

(b) The differences of the two-axle model from the exact model (with damping) are very small (from 0·20 to 1·50%). Thus one can consider that the two-axle model is satisfactorily accurate.

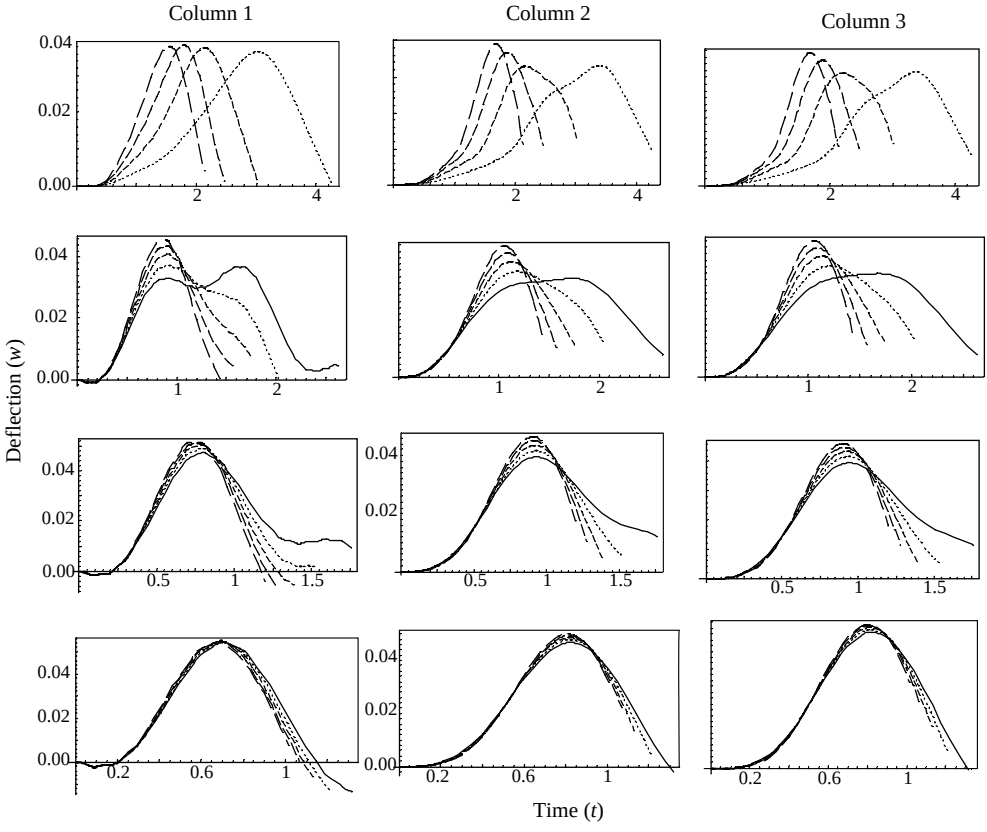

Figure 3. Relationship between the dimensionless deflections w(0·5, t) to the dimensionless time, for various dimensionless velocities and for the one-axle load (column 1), two-axle vehicle (column 2) and two-axle model with damping (column 3). Accelerating movement: (——, $\bar{\gamma} = 0$; · · · · · ·, $\bar{\gamma} = 0{\cdot}11$; - - -, $\bar{\gamma} = 0{\cdot}22$; — — —, $\bar{\gamma} = 0{\cdot}33$; ——, $\bar{\gamma} = 0{\cdot}44$) with $v = 0$ m/s (row 1), $v = 0{\cdot}38$ m/s (row 2), $v = 0{\cdot}57$ m/s (row 3) and $v = 0{\cdot}76$ m/s (row 4).

(c) By studying the accelerating movement (Table 1 and Figure 3), of the two-axle model, one can see that the differences from a movement with constant speed are higher than 7% and one often meets differences of 20 to 33%.

(d) As for the decelerating movement (Table 2 and Figure 4), the differences (for the two-axle model also) from a movement with constant speed amount from −27 to +4%.

One sees that the accelerating movement tends to induce larger bridge deflections, while the decelerating movement smaller ones.

4. CONCLUSION

On the basis of the chosen model, one can draw the conclusions:

(1) The effect of a variable speed is significant for the deflections of the bridge.

(2) The loading by a two-axle model is more accurate than that by a single-axle model.

(3) The influence of the external (usual) damping can be neglected.

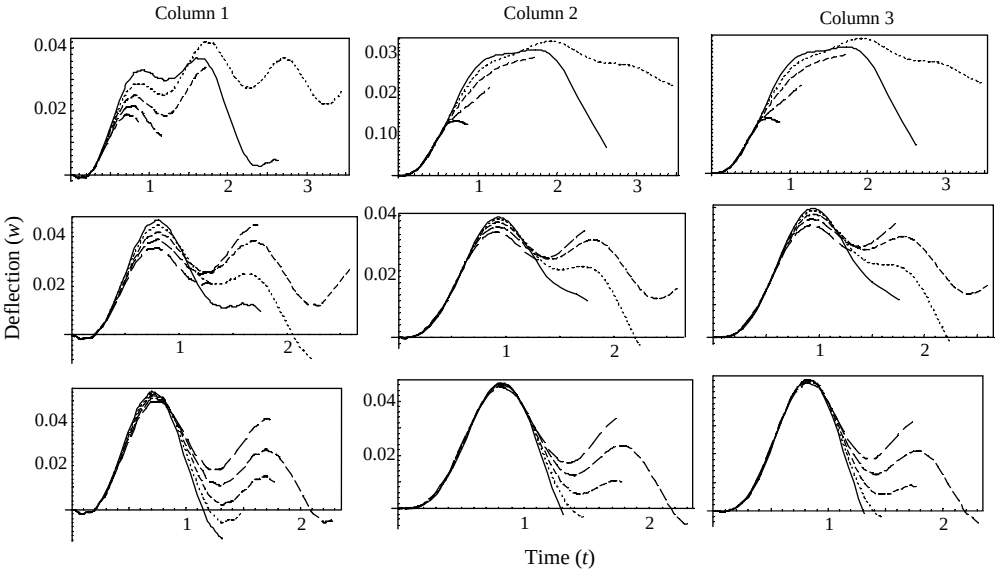

Figure 4. Relationship between the dimensionless deflections $w(0{\cdot}5,\ t)$ to the dimensionless time, for various dimensionless velocities and for the one-axle load (column 1), two-axle vehicle (Column 2) and two-axle model with damping (column 3). Decelerating movement: (——, $\bar{\gamma} = 0$; ⋯⋯, $\bar{\gamma} = 0{\cdot}11$; - - -, $\bar{\gamma} = 0{\cdot}22$; – – –, $\bar{\gamma} = 0{\cdot}33$; ——, $\bar{\gamma} = 0{\cdot}44$) with $v = 0{\cdot}38$ m/s (row 1), $v = 0{\cdot}57$ m/s (row 2) and $v = 0{\cdot}76$ m/s (row 3).

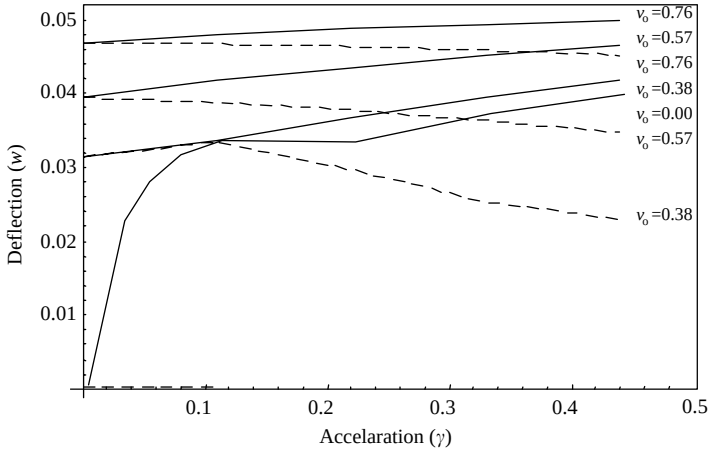

Figure 5. Relationship between the dimensionless deflections $w(0.5,\ t)$ to the dimensionless accelerations (continuous lines) or decelerations (dashed lines) for various dimensionless initial velocities.

REFERENCES

1. G. Stokes 1849 *Transactions of the Cambridge Philosophical Society* (Part 5) 707–735. Discussion of a differential equation relating to the breaking of railway bridges. (reprinted in: Mathematical and Physical Papers, 1883, 178–220).
2. H. Zimmermann 1896 *Centralblatt der Bauverwaltung* **16**, 249–251, 257–260, 264–266, 288. Die Schwingungen eines Tragers mit bewegter Lasts.
3. A. N. Krylov 1905 Mathematical Collection of Papers of the Academy of Sciences, Vol. 61. Matematischeskii sbornik Akademii Nauk; A. N. Peterburg Kriloff. Mathematische Annalen. Uber die erzwungenen Schwingungen von gleichformigen elastischen Staben.

4. S. P. Timoshenko 1908 *Izvestiya Kievskogo Politekhnicheskogo Instituta*. Forced vibration of prismatic bars (in Russian). Also 1911, *Zeitschrift fuer Mathematik und Physik* **59**, 163–203. Erzwungene Schwingungen prismatischer Stabe (in German).
5. A. N. Lowan 1935 *Philosophical Magazine*, *Series* 7 **19**, 708–715. On transverse oscillations of beams under the action of moving variable loads.
6. H. Steuding 1934 *Ingenieur-Archiv* 275–305, 265–270. Die Schwingungen von tragern bei bewegten lasten. I, II.
7. A. Schallenkamp 1937 *Ingenieur-Archiv* **8**, 182–198. Schwingungen von tragern bei bewegten lasten.
8. V. V. Bolotin 1961 *Izvestiya AN SSSR, Mekhanika I Mashinostroenie* Vol. 4, 109–115. Problem of bridge vibration under the action of a moving load (in Russian).
9. C. E. Inglis 1934 *A Mathematical Treatise on Vibration in Railway Bridges*. Cambridge: The University Press.
10. A. Hillerborg Ed. 1951 *Kungliqa Tekn. Hogskolan, Stockholm*. Dynamic influences of smoothly running loads on simply loads on simply supported girders.
11. J. M. Biggs, H. S. Suer and J. M. Louw 1959 *Transactions of the American Society of Civil Engineers* **124**, 291–318. Vibration on simple-span highway bridges.
12. S. P. Timoshenko 1953 *History of the Strength of Materials*. New York: D. van Nostrand Co.
13. V. Kolousek 1967, 1956, 1961 *Dynamics of Civil Engineering Structures. Part I—General Problems, second edition; Part II—Continuous Beams and Frame Systems, second edition; Part III—Selected topics* (in Czech.). Prague: SNTL
14. L. Fryba 1972 *Vibration of Solids and Structures Under Moving Loads*. Research Institute of Transport. Prague.
15. L. Fryba 1976 *Journal of Sound and Vibration* **46**, 323–338. Non-stationary response of a beam to a moving random force.
16. L. Fryba 1980 *Journal of Sound and Vibration* **70**, 527–541. Estimation of fatigue life of railway bridges under traffic loads.
17. A. S. Veletsos and T. Huang 1971 *Journal of Engineering Mechanic Division* **96**, 593–620. Analysis of dynamic response of Hoghway Bridges.
18. G. T. Michaltsos, D. Sophianopoulos and A. N. Kounadis 1996 *Journal of Sound and Vibration* **191**, 357–362. The effect of a moving mass and other parameters on the dynamic response of a simply supported beam.
19. D. G. Fertis 1987 *Proceedings Structures Congress '87/ST.DIV/ASCE, Orlando FL,* 449–468. Safety of long span Highway bridges based on dynamic response.
20. M. Abdel-Rohman and J. Al Duaij 1996 *Computers and Structures* **59**, 291–299. Dynamic response of hinged-hinged single span Bridges with uneven deck.
21. G. T. Michaltsos and T. G. Konstantakopoulos 2000 *Journal of Vibration and Control* **6**, 667–689. Dynamic response of a bridge with surface deck irregularities.
22. G. T. Michaltsos and A. N. Kounadis 2001 *Journal of Vibration and Control* **7**, 315–326. The effects of centripetal and coriolis forces on the dynamic response of light bridges under moving loads.
23. H. S. Zibdeh 1995 *Engineering Structures* **17**, 530–535. Stochastic vibration of an elastic beam due to random moving loads and deterministic axial forces.

APPENDIX A

Numerical results are obtained by using the formulae:

$$\int_0^t \sin(a\tau + b\tau^2)\sin[\omega(t-\tau)]\,\mathrm{d}\tau$$

$$= \sqrt{\frac{\pi}{8b}}\left(\cos\left(\frac{(a-\omega)^2}{4b} - t\omega\right)\mathrm{FresC}\left[\frac{a-\omega}{\sqrt{2\pi b}}\right] - \cos\left(\frac{(a-\omega)^2}{4b} - t\omega\right)\mathrm{FresC}\left[\frac{a+2bt-\omega}{\sqrt{2\pi b}}\right]\right.$$

$$\left. - \cos\left(t\omega + \frac{(a+\omega)^2}{4b}\right)\mathrm{FresC}\left[\frac{a+\omega}{\sqrt{2\pi b}}\right] + \cos\left(t\omega + \frac{(a+\omega)^2}{4b}\right)\mathrm{FresC}\left[\frac{a+2bt+\omega}{\sqrt{2\pi b}}\right]\right.$$

$$+\sin\left(\frac{(a-\omega)^2}{4b}-t\omega\right)\mathrm{FresS}\left[\frac{a-\omega}{\sqrt{2\pi b}}\right]-\sin\left(\frac{(a-\omega)^2}{4b}-t\omega\right)\mathrm{FresS}\left[\frac{a+2bt-\omega}{\sqrt{2\pi b}}\right]$$
$$-\sin\left(t\omega+\frac{(a+\omega)^2}{4b}\right)\mathrm{FresS}\left[\frac{a+\omega}{\sqrt{2\pi b}}\right]+\sin\left(t\omega+\frac{(a+\omega)^2}{4b}\right)\mathrm{FresS}\left[\frac{a+2bt+\omega}{\sqrt{2\pi b}}\right]\Bigg)$$

$$\int_0^t \sin(a\tau+b\tau^2)\sin[\omega(t-\tau)]e^{-c(t-\tau)}\,\mathrm{d}\tau$$
$$=\frac{(-1)^{3/4}\sqrt{\pi}\mathrm{e}^{-iA}}{8\sqrt{b}}\Bigg(-\mathrm{e}^{\mathrm{i}B}\,\mathrm{erf}\,\mathrm{i}\left[\frac{(-1)^{1/4}(c-\mathrm{i}a+\mathrm{i}\omega)}{2\sqrt{b}}\right](\sin t\omega+\mathrm{i}\cos t\omega)$$
$$+\mathrm{e}^{\mathrm{i}\Gamma}\,\mathrm{erf}\,\mathrm{i}\left[\frac{(-1)^{3/4}(a+2bt+\omega+\mathrm{i}c)}{2\sqrt{b}}\right](-\sin t\omega+\mathrm{i}\cos t\omega)$$
$$+\mathrm{e}^{\mathrm{i}\Delta}\,\mathrm{erf}\,\mathrm{i}\left[\frac{(-1)^{3/4}(c+\mathrm{i}a+\mathrm{i}\omega)}{2\sqrt{b}}\right](-\cos t\omega+\mathrm{i}\sin t\omega)$$
$$+\mathrm{e}^{\mathrm{i}\Delta}\,\mathrm{erf}\,\mathrm{i}\left[\frac{(-1)^{1/4}(a+2bt+\omega+\mathrm{i}c)}{2\sqrt{b}}\right](-\cos t\omega+\mathrm{i}\sin t\omega)$$
$$+\mathrm{e}^{\mathrm{i}B}\,\mathrm{erf}\,\mathrm{i}\left[\frac{(-1)^{1/4}(-\mathrm{i}a-2\mathrm{i}bt+c+\mathrm{i}\omega)}{2\sqrt{b}}\right](\sin t\omega+\mathrm{i}\cos t\omega)$$
$$+\mathrm{e}^{\mathrm{i}E}\,\mathrm{erf}\,\mathrm{i}\left[\frac{(-1)^{3/4}(c+\mathrm{i}a-\mathrm{i}\omega)}{2\sqrt{b}}\right](\cos t\omega+\mathrm{i}\sin t\omega)$$
$$+\mathrm{e}^{\mathrm{i}E}\,\mathrm{erf}\,\mathrm{i}\left[\frac{(-1)^{3/4}(\mathrm{i}a+2\mathrm{i}bt+c-\mathrm{i}\omega)}{2\sqrt{b}}\right](\cos t\omega+\mathrm{i}\sin t\omega)$$
$$+\mathrm{e}^{\mathrm{i}\Gamma}\,\mathrm{erf}\,\mathrm{i}\left[\frac{(-1)^{3/4}(a+\omega+\mathrm{i}c)}{2\sqrt{b}}\right](\sin t\omega+\mathrm{i}\cos t\omega)\Bigg),$$

where

$$A=(a^2+c^2+\omega^2+2a(\omega-\mathrm{i}c)-2\mathrm{i}c(2bt+\omega))/4b,\quad B=(a^2-2\mathrm{i}c\omega+\omega^2)/2b,$$
$$\Gamma=(a+\omega)^2/2b,\quad \Delta=c^2/2b,\quad E=(c^2+2a\omega-2\mathrm{i}c\omega)/2b$$

and

$$\mathrm{FresS}[z]=\int_0^z \sin(\pi t^2/2)\,\mathrm{d}t,\quad \mathrm{FresC}[z]=\int_0^z \cos(\pi t^2/2)\,\mathrm{d}t,$$
$$\mathrm{erf}[z]=\frac{2}{\sqrt{\pi}}\int_0^z \mathrm{e}^{-t^2}\,\mathrm{d}t$$

are the Fresnel integrals S[z], and C[z] while erf[z] is the integral of the Gaussian distribution (error function) respectively.